Preparation and Properties of Poly(vinyl acetate)/Silica-Gel Microhybrids

SHOICHIRO YANO,[1] KENSUKE NAKAMURA,[2] MITSUO KODOMARI,[2] and NAOFUMI YAMAUCHI[3]

[1]National Institute of Materials and Chemical Research, 1-1 Higashi, Tsukuba-shi, Ibaraki 305, Japan; [2]Shibaura Institute of Technology, 3-9-14, Shibaura, Minato-Ku, Tokyo 108, Japan; and [3]Seiko Instruments Inc., 563 Takatsuka-shinden, Matsudo-shi Chiba 271, Japan.

SYNOPSIS

Poly(vinyl acetate) (PVAc) was incorporated into silica gel using the sol–gel process involving tetraethoxysilane (TEOS). In order to prepare silica-gel microhybrids, two different processes were employed, and the physical properties of the resulting two sets of hybrids were compared. In the first method, PVAc was first mixed with TEOS in an acetone solution and then cured using HCl and H_2O. In the second method, an acetone solution of a copolymer composed of vinyl acetate (VAc) and vinyl triethoxysilane (VTES) was first mixed with TEOS and then cured. This copolymer contained 10 mol % of VTES component and was bound covalently to silica-gel molecules. When comparing the properties of the hybrids, the dynamic modulus, E', increased with increasing amounts of TEOS over a wide temperature range: −20–120°C. E' of a hybrid from PVAc was lower than that of a hybrid from the VAc/VTES copolymer. A sharp peak in the loss modulus, E'', of a PVAc hybrid occurred at 40°C, and its position did not change with TEOS content. In contrast, the E'' peak of a copolymer hybrid was broad and its position also shifted to a higher temperature as the TEOS content increased. The tensile strength of a PVAc hybrid increased as the amount of mixed TEOS increased, reaching a maximum of 30 MPa at 50 wt % of TEOS. However, the strength of a copolymer hybrid reached a maximum of 50 MPa at 50 wt % of TEOS. The differences in the physical properties between a PVAc hybrid and a copolymer hybrid arise from the difference in their structure. Organic polymer molecules in a copolymer hybrid combine covalently with silica-gel molecules through the VTES component, while a PVAc hybrid has no bonding between PVAc and silica-gel molecules. © 1994 John Wiley & Sons, Inc.

INTRODUCTION

In recent years, composite materials having microstructure have been investigated in the fields of metals, ceramics, and polymers in order to develop high-performance and highly functional materials.[1] Organic polymer blends, such as polymer alloys and molecular composites, are typical microcomposites with nano-order microstructures and are successfully used, for example, in the automotive industry.

By using the sol–gel process involving metallic alkoxides, organic polymers can be incorporated into inorganic polymers (i.e., ceramics) yielding molecular level composites which are called microhybrids. Saegusa[2] prepared a microhybrid using the sol–gel reaction of tetraethoxysilane (TEOS) in the presence of an organic polymer having an N-alkylamide group, thus establishing a molecular level dispersion (10–20 Å) of the organic polymer in a silica-gel matrix. In this case, it is believed that hydrogen bonding occurs between the organic polymer and a silanol group in the silica gel. Poly(vinyl alcohol)/alumina-gel microhybrids have been fabricated by using the sol–gel process involving aluminum isopropoxide, resulting in transparent composites.[3] Nandi and coworkers[4] obtained polyimide films containing homogeneous dispersion of either SiO_2 or TiO_2 particles 1–1.5 nm in size using the sol–gel process. In order to reinforce a weak elastomer, 250 Å silica

Journal of Applied Polymer Science, Vol. 54, 163–176 (1994)
 CCC 0021-8995/94/020163-14

particles were dispersed in poly(dimethylsiloxane) using the sol–gel process.[5–7] Recently, various kinds of microhybrids have been investigated; e.g., polyethyleneglycol(PEG)/SiO_2,[8] poly(tetramethyleneoxide) (PTMO)/TiO_2, ZrO_2,[9] PTMO/Al_2O_3,[10] PTMO/SiO_2,[11,12] poly(*n*-butyl methacrylate)/TiO_2,[13] poly(methyl methacrylate)/SiO_2,[14] and perfluorosulfonic acid ionomer/SiO_2.[15]

Nakanishi et al.[16] have reported that in the case of a sodium polystyrene sulfonate (NaPSS)/SiO_2 microhybrid, the domain formation due to the microphase separation occurred during gelation. The domain size ranged from about 0.2 to 50 nm, depending on the starting composition of the sample sols (i.e., polymer and water concentrations) and curing temperature. Matsuoka and co-workers[17] investigated the small-angle x-ray scattering (SAXS) of a NaPSS/SiO_2 hybrid during gelation process. The apparent radius of gyration, Rg, which can be evaluated by the Guinier law, increased with gelation time and reached about 200 Å. They have reported that the sol–gel transition was accelerated by the presence of the polymer and that the microphase separation into a silica-rich phase and a polymer-rich phase occurred.

In order to avoid phase separation, the organic species to be incorporated in the network must be functionally reactive with silicon alkoxide precursor during the course of the sol–gel reaction.[18] Wilkes and co-workers have successfully incorporated PTMO based polyurethane oligomers with multiple triethoxysilane groups into a TEOS-based silicate network.[19] They also used an amine-terminated amorphous poly(arylene ether)ketone, endcapped with isocyanatopropyl triethoxy silane, to synthesize a hybrid network with TEOS.[20] To evaluate the morphology of these microhybrids using SAXS, a correlation length of the order of 10 nm was calculated.[19,20] Fujita and Honda prepared poly(ethylene oxide)(PEO)/SiO_2 microhybrid using PEO endcapped with bis(3-silylpropyl)ethers, and developed an ion conductive hybrid that has a conductivity on the order of 10^{-3} S·cm^{-1}.[21,22]

In this study, poly(vinyl acetate) (PVAc) was incorporated into a silica-gel network by two different processes, and the physical properties of the obtained hybrids were compared. The first method involved PVAc dissolved in acetone that was mixed with TEOS. The mixture was then hydrolyzed and polycondensed using H_2O and HCl. In the second method, a copolymer of vinyl acetate (VAc) and vinyl(triethoxysilane) (VTES) was prepared, and an acetone solution of the copolymer was mixed with TEOS. The mixture was then polycondensed after hydrolysis. The copolymer was incorporated into the silica-gel network through the chemical reaction of TEOS and ethoxyl groups in the copolymer.

EXPERIMENTAL

Materials

The VAc monomer was supplied by Wako Pure Chemical Industries, Ltd., and before polymerization it was purified by distillation at about 73°C at atmospheric pressure. The VTES monomer was supplied by Chisso Co. Ltd., and was used after distillation at 63°C at 20 mmHg. The TEOS was supplied by Shin-etsu Chemical Industries Ltd., and was used without further purification.

Polymerization

Polymerization of VAc was carried out as follows. First, 100 g of VAc and 1 g of 2,2′-azobis(isobutyronitrile) (AIBN) were dissolved in 150 g of benzene. The mixture was then heated and stirred at the reflux temperature of benzene (77°C) for 5 h. The polymer was then precipitated in hexane and dried *in vacuo* at room temperature.

The viscosity-average molecular weight M_V was 60,000, which was estimated at 30°C in benzene by Equation (1).[23]

$$[\eta] = 5.63 * 10^{-3}\, Mv^{0.62} \qquad (1)$$

where $[\eta]$ is the intrinsic viscosity.

Poly(vinyltriethoxysilane) homopolymer was obtained by heating and stirring a mixture of 5 g of VTES monomer, 0.5 g of AIBN, and 15 g of benzene at 77°C for 15 h.

Copolymerization of VAc and VTES was carried out in such a way that the total amount of VAc and VTES monomer mixture, namely 10 g, was dissolved in 20 g of benzene together with 0.2 g of AIBN. The resulting mixture was heated at 77°C for 15 h. The copolymer thus obtained was purified by eliminating benzene and the VAc monomer by distillation at 90°C at atmospheric pressure, and then removing the VTES monomer by distillation at 90°C at 30 mmHg. The mole ratios of VAc : VTES in the copolymers were 9 : 1, 8 : 2, and 5 : 5, which were determined by using a composition curve as shown in Figure 1. The composition curve was calculated by using the $Q - e$ scheme as follows. Since $Q_1 = 0.026$ and $e_1 = -0.220$ for VAc, and $Q_2 = 0.03$ and $e_2 = 0.100$ for VTES have been reported,[24] the

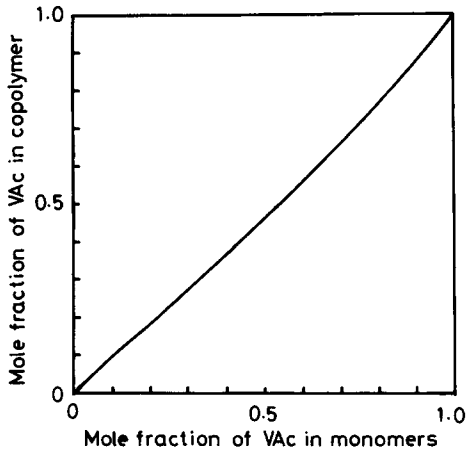

Figure 1 Instantaneous composition of a copolymer as a function of monomer composition for a VAc/VTES copolymer.

monomer reactivity ratios can be calculated as Equations (2) and (3).[25]

$$r_1 = (Q_1/Q_2)\exp\{-e_1(e_1 - e_2)\} \quad (2)$$

$$r_2 = (Q_2/Q_1)\exp\{-e_2(e_2 - e_1)\} \quad (3)$$

Concentrations of VAc and VTES in a copolymer, $d[M_1]$ and $d[M_2]$, respectively, are calculated from the concentrations of VAc and VTES in a monomer mixture, $[M_1]$ and $[M_2]$:

$$d[M_1]/d[M_2] = ([M_1]/[M_2]) * \{([M_1] + r_2[M_2])/(r_1[M_1] + [M_2])\} \quad (4)$$

The mole fraction of VAc in a copolymer, F_1, and that in monomer mixture, f_1, are then given by

$$F_1 = d[M_1]/(d[M_1] + d[M_2]) \quad (5)$$

$$f_1 = [M_1]/([M_1] + [M_2]) \quad (6)$$

The yields of the copolymers 9/1, 8/2, and 5/5 were 80, 65, and 50%, respectively. The $[\eta]$ in benzene at 30°C for these same copolymers were 0.11, 0.085, and 0.058, respectively.

Preparation of Microhybrids

A 20% acetone solution of PVAc homopolymer or copolymer was mixed with TEOS, HCl, and H_2O, and stirred by using ultrasonic waves. The mole ratios of H_2O and HCl to TEOS were defined as 4 and 0.1, respectively. The weight fractions of TEOS in the mixture were varied, namely 20, 40, 50, 60, and 80%. The mixture was poured into a petri dish, left to dry at room temperature for 5 days, and then cured at 60°C for a week. When the TEOS contents was less than 60%, a yellowish and transparent free-standing film was obtained. On the other hand, beyond 60% a free-standing film was not yielded. The nomenclature used hereafter for the hybrids from PVAc mixed with 20, 40, 50, 60, and 80% of TEOS is VA-20, VA-40, VA-50, VA-60, and VA-80, and the hybrids from copolymer 9/1 mixed with 20, 40, 50, 60, and 80% are labeled as CO-20, CO-40, CO-50, CO-60, and CO-80, respectively.

Measurements

Infrared spectra were taken and recorded with a Nicolet 20 DXB FT-IR spectrometer. The homopolymers and copolymers were deposited from a benzene solution on a KBr plate that was 5 mm thick and 30 mm in diameter.

The thermogravimetry (TG) and differential scanning calorimetry (DSC) of PVAc, copolymers, and hybrids were measured using Seiko TG/DTA 320 and DSC 220 (Seiko Instruments, Inc.) at a heating rate of 10°C/min in a nitrogen atmosphere.

The tensile properties were measured using a Tensilon UTM II (Orientec Co., Ltd.) at 25°C and 50% relative humidity. The crosshead speed was 10 mm/min and the gauge length was 10 mm. Rectangular test specimens (5 mm wide and about 0.2 mm thick) were used for determining the stress–strain behavior to failure.

The dynamic viscoelastic properties of PVAc and the hybrids were measured using a Rheograph Solid (Toyoseiki Manufacturing Co., Ltd.) at a heating rate of 2°C/min and a frequency of 100 Hz in a nitrogen atmosphere. Rectangular specimens used were 5 mm by 0.2 mm and 30 mm long.

RESULTS AND DISCUSSION

Characterization of PVAc, PVTES, and the VAc/VTES Copolymers

Figure 2 shows IR spectra of PVAc, PVTES, and the VAc/VTES copolymers. Copolymers with a VAc/VTES mole fraction of 9/1, 8/2, and 5/5 were used, hereafter labeled CP 9/1, CP 8/2, and CP 5/5, respectively. PVAc has strong peaks at 1235 cm^{-1} (corresponding to C—O—stretching vibration in ester) and 1730 cm^{-1} (C=O stretching vibration), and weak peaks at around 2900–3000 cm^{-1}. A peak

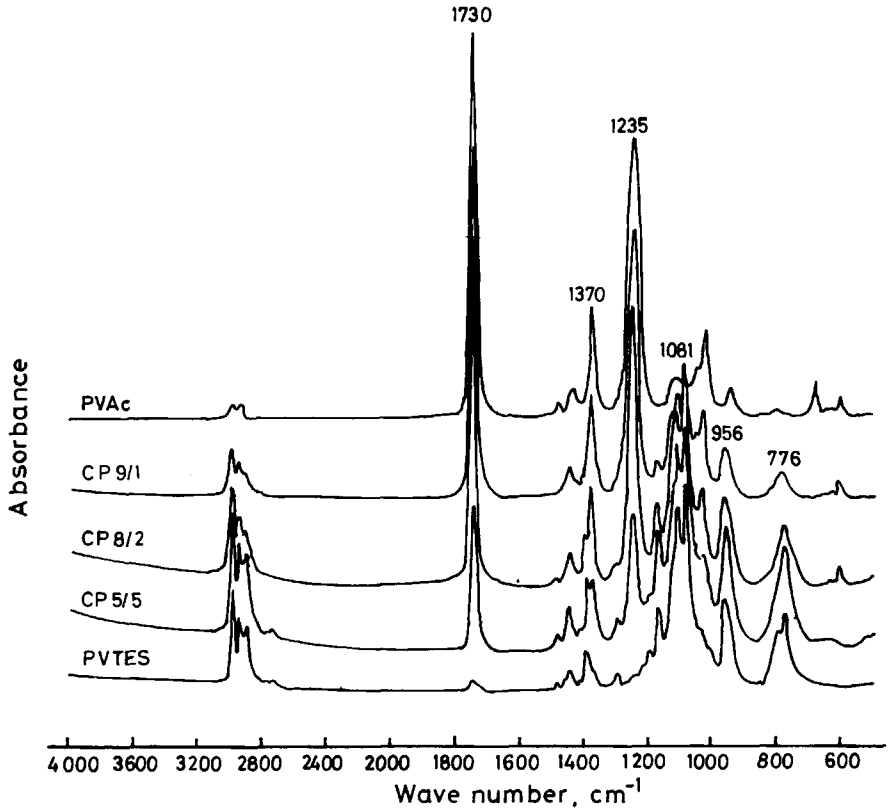

Figure 2 Infrared spectra for PVAc, PVTES, and the VAc/VTES copolymers.

at 776 cm^{-1} may also be due to the stretching vibration of the Si—C link. The copolymers have peaks that combine those of PVAc and PVTES. As the VAc component in the copolymer decreases, we see a progressive increase in the peaks at 1080–1100 cm^{-1} and a decrease at 1730 cm^{-1} and 1235 cm^{-1}.

Figure 3 shows the thermogravimetry (TG) of PVAc, PVTES, and the copolymers. A two-stage

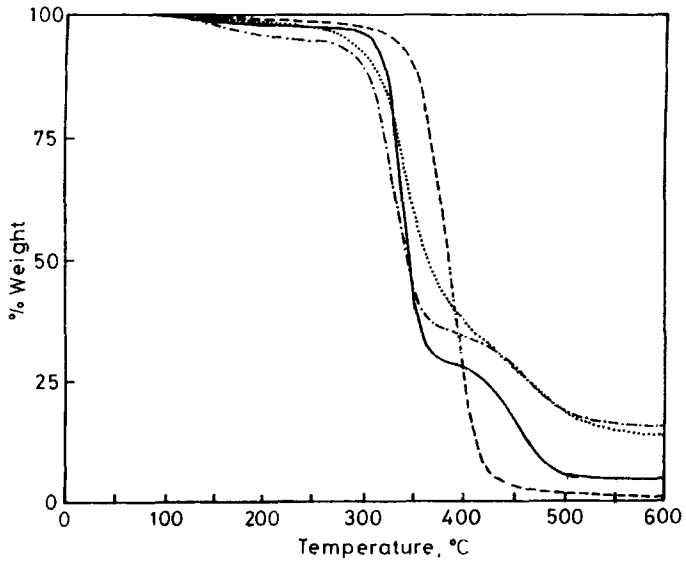

Figure 3 TG curves of PVAc (——), PVTES (----), CP 9/1 (-·-), and CP 5/5 (·····).

degradation is seen in the weight loss curve of PVAc. The first drop at about 280°C is caused by the removal of acetic acid, and the second drop at 400°C is due to the breakup of a —(C=C)n— chain formed after the elimination of acetic acid.[26] The residual percent weight of PVAc at 600°C was about 5%. In the case of PVTES, a one-stage degradation occurred, with weight loss starting at about 350°C (which was higher than that for PVAc) and a residual weight of 0.6%. The weight loss of CP 9/1 showed a two-stage degradation due to the influence of 90 mole % of the VAc component. The first stage occurred at about 272°C and the second at about 430–450°C. The TG behavior of CP 5/5 was slightly different from that of CP 9/1 in that the initial stage began at about 260°C, but the second, at about 400°C, was not sharp because of the increased amount of VTES component. The residual weights of both copolymers were about 15%, larger than those of PVAc and PVTES.

Figure 4 shows DSC curves for PVAc, PVTES, and the copolymers. A clear endothermic change due to the glass transition temperature is seen for every polymer. If the onset of the endothermic change is defined as the glass transition temperature (Tg) of a polymer (indicated by arrows in Fig. 4), Tgs of the polymers are then −79.8, −57.9, −15.4, −5.1, and 17.2°C for PVTES, CP 5/5, CP 8/2, CP 9/1, and PVAc, respectively. Equations for the variation of Tg with copolymer composition have been proposed by many researchers, e.g., Gordon and Taylor,[27] Fox,[28] Manderkern et al.,[29] and Wood.[30] Wood's equation is simple:

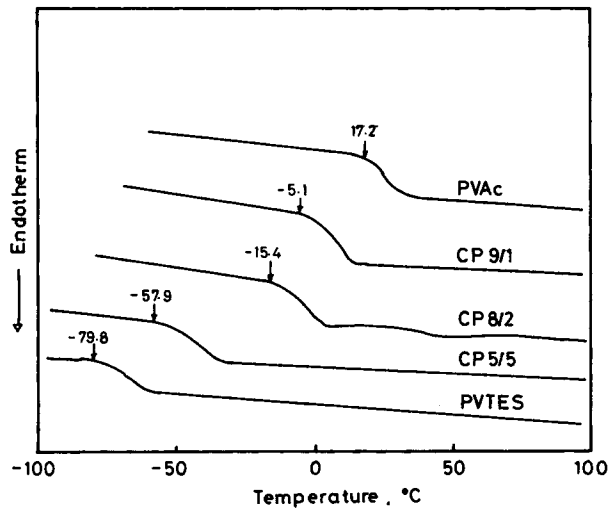

Figure 4 DSC curves of PVAc, PVTES, CP 9/1, CP 8/2, and CP 5/5.

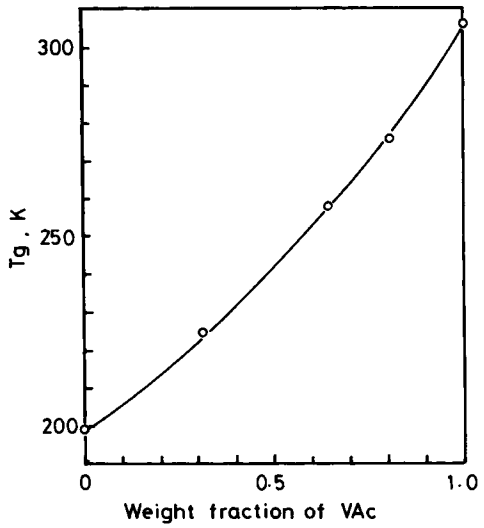

Figure 5 Relationship between the glass transition temperature and weight fraction of VAc in a copolymer using experimental data and Wood's equation.

$$(1/\mathrm{Tg}) = (W_1/Tg_1) + (W_2/Tg_2) \qquad (7)$$

where Tg is the glass transition temperature of the copolymers, Tg_1 and Tg_2 are Tgs of the homopolymers 1 and 2, and W_1 and W_2 are the weight fractions of each of the components of the copolymer. Figure 5 shows the relation between Tg of the homopolymers and the copolymers and the weight fraction of VAc in the copolymers obtained both experimentally (open circle) and by using Wood's equation (solid line). The weight fraction of VAc was converted from the mole fraction of the copolymer. As we can see, Wood's equation represents the experimental data fairly well.

In order to prepare silica-gel microhybrids, CP 9/1, CP 8/2, and CP 5/5 were mixed with 20 wt % of TEOS and cured at room temperature for 5 days and at 60°C for a week. Because molecular weights of organic chains between crosslinks became small, the microhybrids from CP 8/2 and CP 5/5 were too brittle to obtain free-standing films. In the case of CP 9/1, yellowish and transparent free-standing films were obtained, even when it was mixed with 50 wt % of TEOS.

Thermal Properties of Microhybrids

Silica-gel microhybrids of PVAc and CP 9/1 were produced by mixing TEOS via the sol–gel process (described in the Experimental section). Figure 6 shows TG curves of PVAc and its microhybrids, VA-

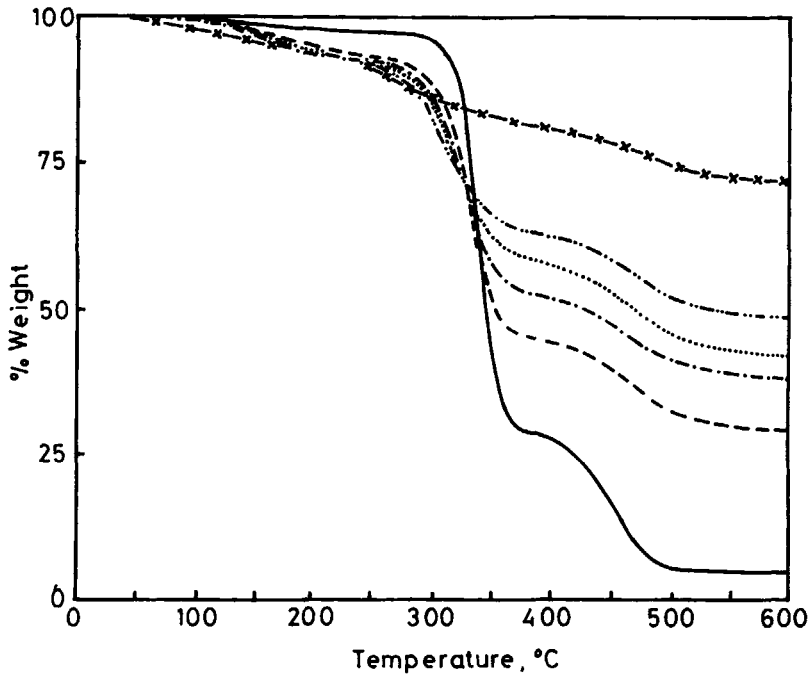

Figure 6 TG curves of PVAc (——), VA-20 (----), VA-40 (– · –), VA-50 (· · · · ·), VA-60 (– · · –), and VA-80 (– × –).

20, VA-40, VA-50, VA-60, and VA-80. Two-stage degradation processes are evident, even at an 80% TEOS level with PVAc (microhybrid VA-80). The first decrease in the weight occurred at 280, 270, 265, 262, 258, and 235°C for PVAc, VA-20, VA-40, VA-50, VA-60, and VA-80, respectively. As the amount of mixed TEOS increased, the onset of weight decrease began at a respectively lower temperature. This may be due to the elimination of ethanol and water by the hydrolysis and polycondensation that occurred during the TG measurements. The second-stage process occurred at about 400°C for each sample.

The residual weights at 600°C for PVAc and each hybrid are listed in Table I. Subtraction of the residual weight of PVAc from that of the hybrid should be equal to the amount of silica-gel component in the hybrid, because the residue of PVAc is char while the residue from the hybrid may be a mixture of char and a silica-gel component (i.e., silicate) from the TEOS. Experimental and calculated values of the silicate in the hybrids are also given in Table I. Calculated values were estimated from the amount of TEOS mixed with PVAc (i.e., 20, 40, 50, 60, and 80%), assuming that TEOS was converted completely to silicate (SiO_2). The experimental values were slightly larger than the calculated values because the alkoxysilane groups may not have completely condensed, thus leaving small amounts of silanol groups.

Figure 7 shows the TG curves of CP 9/1 and its hybrids, CO-20, CO-40, CO-50, CO-60, and CO-80. Two-stage degradation processes are evident. The first-stage process occurred at 272, 270, 269, 265, 262, and 231°C for copolymer 9/1, CO-20, CO-40, CO-50, CO-60, and CO-80, respectively. By mixing TEOS with polymers, the onset temperature of the first drastic decrease in the weight was lowered. The second-stage degradation occurred at about 400°C

Table I Silica-Gel Content of PVAc Microhybrids Calculated from Residual Weights of the TG Curves

Sample	Residual Weight %	Silica-Gel Content	
		Experimental %	Calculated %
PVAc	5.4	0	0
VA-20	12.7	7.3	6.7
VA-40	22.5	17.1	16.1
VA-50	29.2	23.8	22.4
VA-60	42.3	36.9	30.2
VA-80	67.2	61.8	53.6

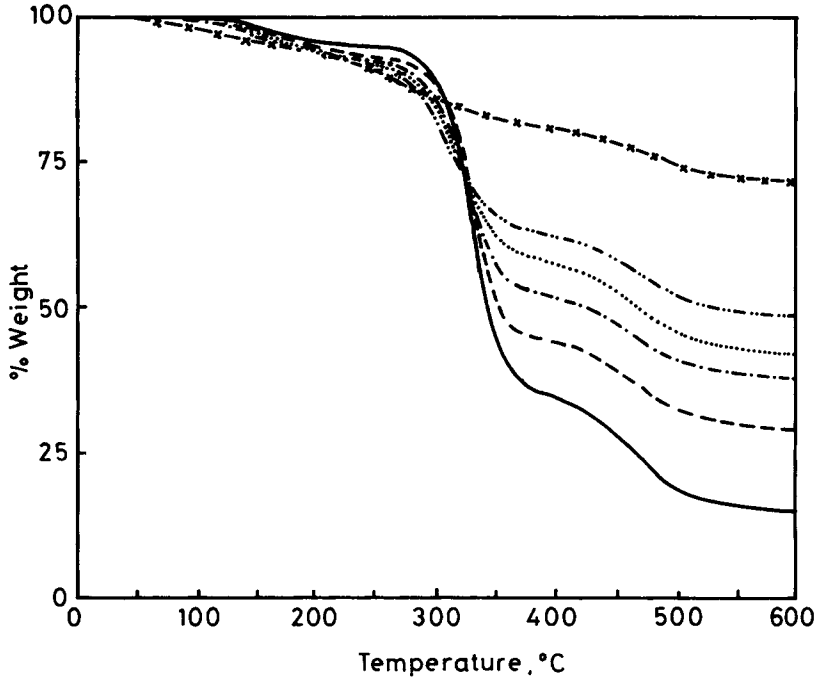

Figure 7 TG curves of CP 9/1 (——), CO-20 (----), CO-40 (– · –), CO-50 (· · · · ·), CO-60 (– · · –), and CO-80 (– × –).

for each sample. The residual weights at 600°C for CP 9/1 and its hybrids are listed in Table II. The residual weight of CP 9/1 was 15%, but this copolymer contains 10 mol % of alkoxysilane component, which corresponds to 6.3 wt % of silicate. Therefore, the carbon residue of CP 9/1 was calculated as 8.7 wt %. The experimental values of the silica-gel content were obtained by subtracting this value of 8.7 wt % from the residual weight of each hybrid, and were found to be larger than the calculated values. This difference between the values may be due to incomplete polycondensation of alkoxysilane.

Table II Silica-Gel Contents of VAc/VTES Copolymer Microhybrids Calculated from Residual Weights of the TG Curves

Sample	Residual Weight %	Silica-Gel Content	
		Experimental %	Calculated %
Copolymer 9/1	15.0	—	6.3
CO-20	29.1	20.4	13.0
CO-40	37.8	29.1	22.4
CO-50	41.8	33.1	28.7
CO-60	48.1	39.4	36.5
CO-80	71.2	62.5	59.9

The DSC results for the silica gel from TEOS, the PVAc hybrid, and CP 9/1 hybrid are displayed in Figures 8, 9, and 10, respectively. In Figure 8, the DSC curve is for silica-gel prepared from TEOS without organic polymer. Because hydrolysis and polycondensation of this silica-gel were incomplete, an exothermic peak appears at 36.9°C due to further hydrolysis, and a broad endothermic peak is observed at 99.0°C, which was caused by elimination of ethanol and water that were formed by polycondensation.

The DSC curves of PVAc and its hybrids, VA-20, VA-40, VA-50, and VA-60, are shown in Figure 9. The second scan is shown in this figure. The first scan was almost the same as the second. For PVAc, an endotherm due to the glass transition began at about 17.2°C. The endotherm of each hybrid began above 30°C. However, a very small exothermic peak which occurred at about 30°C can be attributed to hydrolysis, and the subsequent endotherm broadened because of elimination of ethanol and water that were formed by polycondensation. For the PVAc hybrids, DSC curves between 0 and 100°C are complex because the glass transition behavior of an organic component overlapped the hydrolysis and polycondensation of TEOS.

Figure 10 shows the DSC curves of CP 9/1 and its hybrids, CO-20, CO-40, CO-50, and CO-60. These

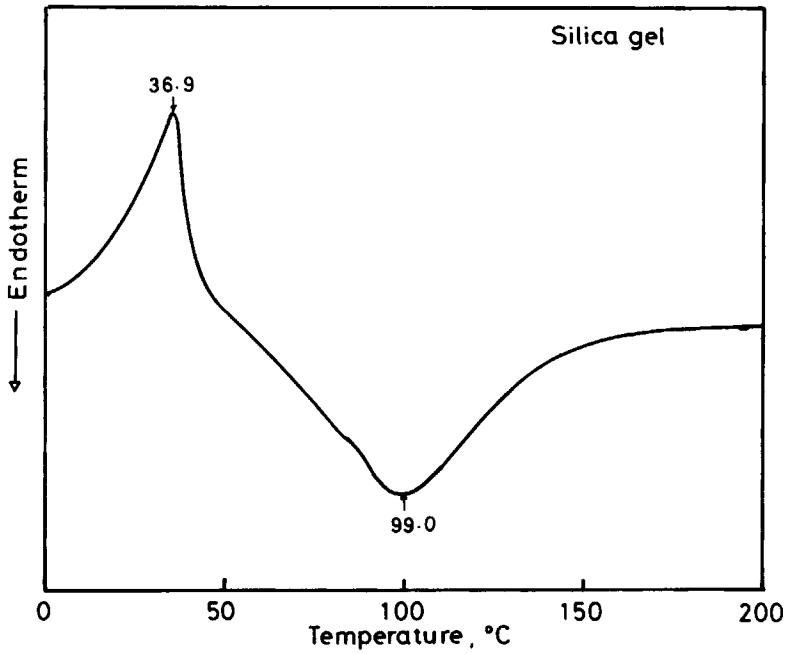

Figure 8 DSC curve of silica-gel prepared from TEOS without an organic polymer.

curves are the second scan. The first scan in this case was complicated, because of the overlapping of an endotherm and an exotherm at around room temperature. An endotherm of CP 9/1 appeared at about 2.2°C. The hybrid, CO-20, had an endotherm at about 32°C, which could be the glass transition of the hybrid due to incorporating the copolymer with silica gel, although condensation may overlap this. CO-40, CO-50, and CO-60 had exothermic peaks at 25.2–26.5°C, accompanied by endotherms,

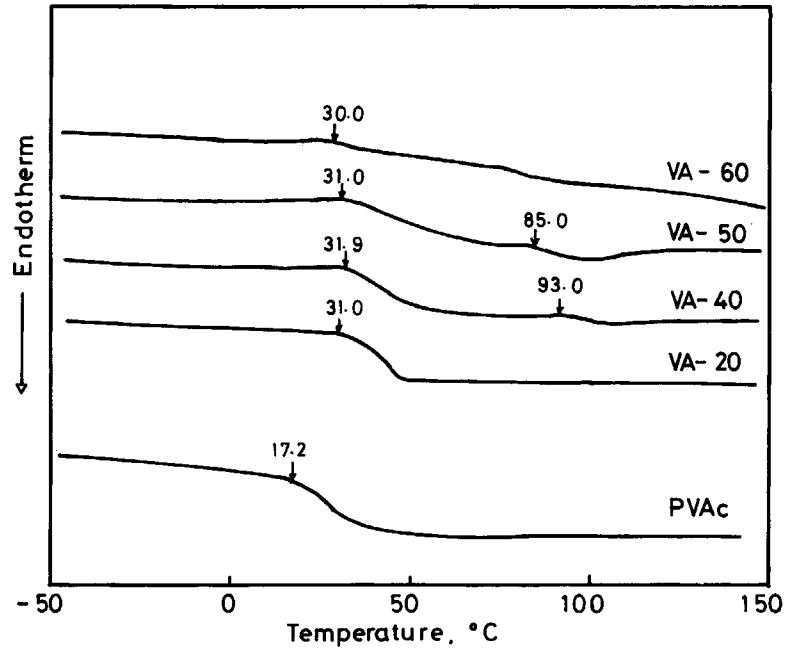

Figure 9 DSC curves of PVAc, VA-20, VA-40, VA-50, and VA-60.

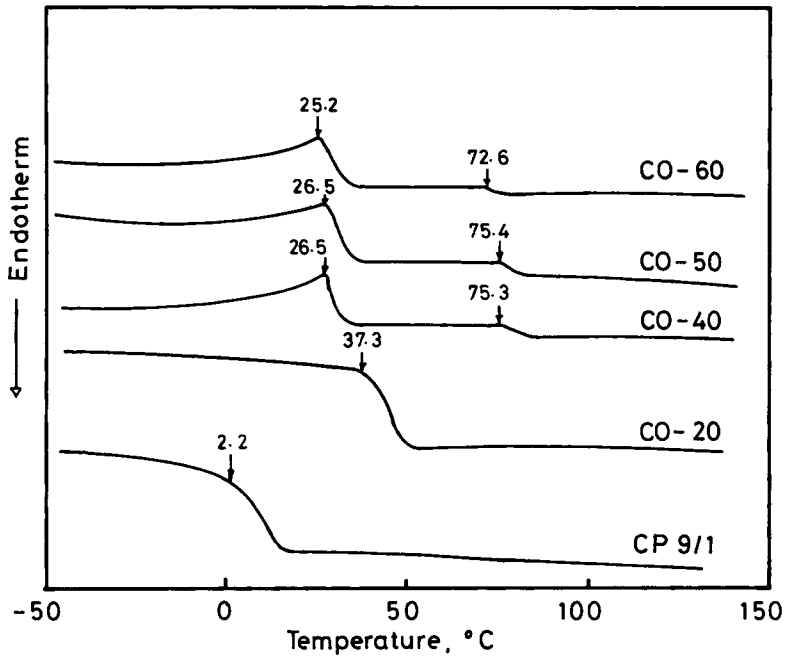

Figure 10 DSC curves of CP 9/1, CO-20, CO-40, CO-50, and CO-60.

that were caused by hydrolysis and polycondensation of ethoxysilane in TEOS and in the VTES component of the copolymer. In the case of the hybrid made of VAc/VTES copolymer and TEOS, a part of the organic chain (i.e., VTES component) is covalently bound to silica gel during the sol–gel process. Therefore, molecular motions of organic chains in these hybrids are strongly restricted by the silicate, causing the Tg of the hybrids to rise. This is confirmed in the DSC endotherm seen at about 73–75°C for CO-40, CO-50, and CO-60. On the other hand, the structure of the hybrid prepared from PVAc and TEOS is much different from that of the copolymer hybrid. Organic molecules in the PVAc hybrid are not bound to the silicate so no significant change in Tg occurs, which is confirmed by our experimental results.

The Mechanical Properties of Microhybrids

Figure 11 shows the temperature dependence of the dynamic viscoelastic properties of PVAc and its hybrids. The dynamic modulus, E' (the upper curves), increased with increasing amounts of mixed TEOS over a wide temperature range: −20–120°C. Above 30°C, E' of PVAc and VA-20 could not be measured because of a drastic decrease in E' due to flow of the samples. VA-40 and VA-50 had a plateau at around 70°C and 80°C, respectively, indicating that the mobility of these hybrids decreases because growth of the silica-gel component prevents flow of the PVAc component incorporated in the silica-gel. The E' of VA-40 and VA-50 had a break point at about 80°C and 90°C, respectively. The lower curves in the figure show the changes in the loss modulus, E'', of PVAc and its hybrids. The E'' of PVAc and VA-20 increased with temperature and had no peak at around Tg because of flow of the samples. In contrast, VA-40 and VA-50 had a large peak at 40°C and a shoulder peak at 60°C and 90°C, respectively. This large peak was caused by the glass transition of the hybrids, and as the amount of TEOS increased, it broadened but did not change its location. The shoulder peak of E'' at 70°C and 90°C for VA-40 and VA-50, respectively, corresponds to the break point in E' that occurred at about 80°C and 90°C, respectively. This relaxation may be identical with that for the endotherm in the DSC curve at around 90°C, as can be seen in Figure 9. However, at present, the origin of this relaxation is uncertain and further investigation into the morphology relating to hybrids is needed.

The dynamic viscoelastic properties of the hybrids made from CP 9/1 are given in Figure 12. The upper curves in the figure compare the temperature dependence of E' for the hybrids CO-20, CO-40, and CO-50 with that for PVAc. This modulus increased with increasing amounts of TEOS, and the slope of the curve for the hybrids mixed with larger amounts of TEOS decreased, especially above Tg. That the

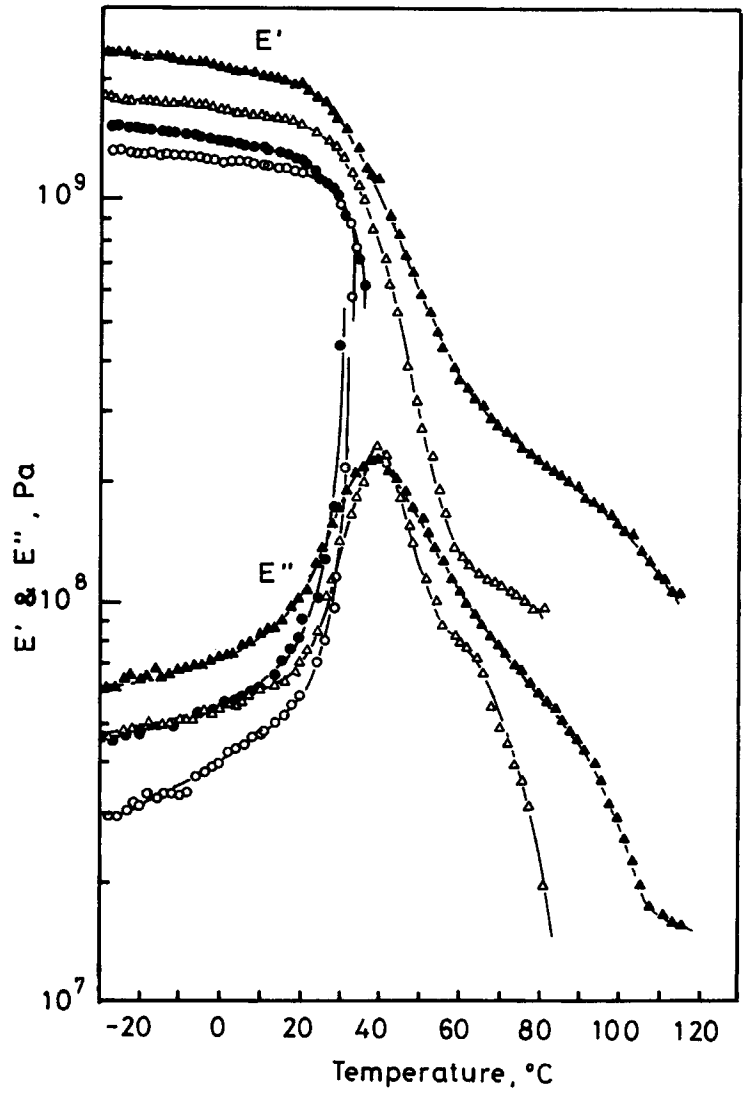

Figure 11 Dynamic viscoelastic properties of PVAc (○), VA-20 (●), VA-40 (△), and VA-50 (▲).

E' values of the CO hybrids were much higher than those of VA hybrids may be due to differences in their structures. Organic polymer molecules in the copolymer hybrid are tightly bound to silica-gel molecules through covalent bonds, while PVAc molecules in the PVAc hybrids are not. The lower curves in Figure 12 compare the changes in E'' of CO hybrids with those of PVAc. Every hybrid had a peak at about 40, 70, and 85°C for CO-20, CO-40, and CO-50, respectively, caused by the glass transition of the hybrid. As the TEOS content increased, the location of this peak shifted to a higher temperature, and the peak broadened, reflecting the structure of the hybrid. When compared with Figure 11, this behavior was much different from VA hybrids.

In Figures 13, 14, and 15, the tensile properties of PVAc and its hybrids are compared. The stress–strain curves of PVAc and its hybrids are shown in Figure 13. PVAc itself had a yield strength at about 7 MPa, a large elongation of 260%, and a very low tensile strength of 6 MPa. The strength of the hybrid increased significantly with increasing amounts of mixed TEOS, although the elongation decreased. The stress–strain behavior of CO hybrids is slightly different from that of VA hybrids as shown in Figure 14 in that the tensile strength of the CP hybrids improved with increasing amounts of TEOS content

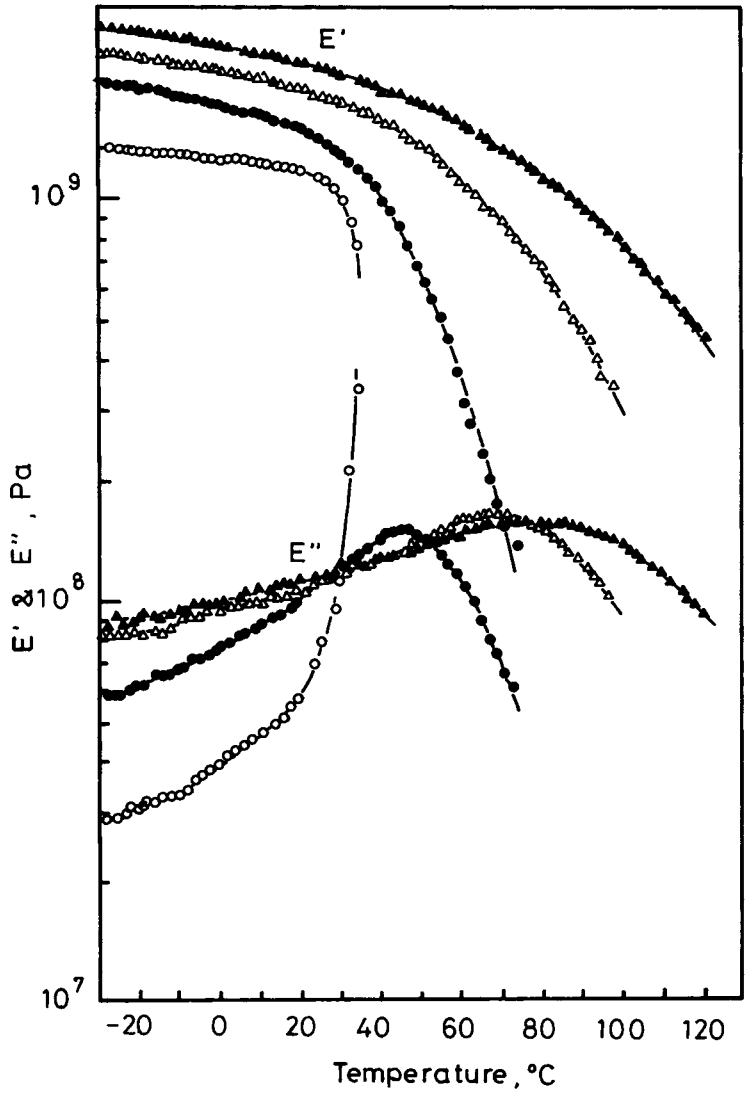

Figure 12 Dynamic viscoelastic properties of PVAc (○), CO-20 (●), CO-40 (△), and CO-50 (▲).

but decreased at 60 wt % of TEOS. CO-60 became very brittle and had the characteristics of a ceramic. The strength of CO hybrids is stronger than that of VA hybrids, resulting from the peculiar structure of the CO hybrids, as described above.

Figure 15, summarizing the tensile properties of both the hybrids, shows that elongation decreased with increasing amounts of TEOS content. Usually, mixing rigid fillers with polymers raises the viscosity of a system and reduces the elongation of a composite. The elongation of a VA hybrid was larger than that of a CO hybrid because the Tgs of VA hybrids (ca 40°C) are lower than those of CO hybrids (50–80°C), as can be seen in Figures 11 and 12. The tensile strengths increased with TEOS content and decreased after reaching a maximum at 50 wt % of TEOS. The maximum strengths were about 30 MPa for VA hybrids and 50 MPa for CO hybrids at 50 wt % of TEOS. Generally, when fillers are mixed *ex situ* and dispersed in polymers, the modulus of elasticity can always be increased, but the strength is reduced with the increase in the filler content because of an increase in the voids between a filler and matrix. However, in the case of microhybrids produced by the sol–gel process, silica gel is incorporated *in situ* with organic polymers and there is covalent crosslinking between the organic matrix and the TEOS species, thus improving the strength. The

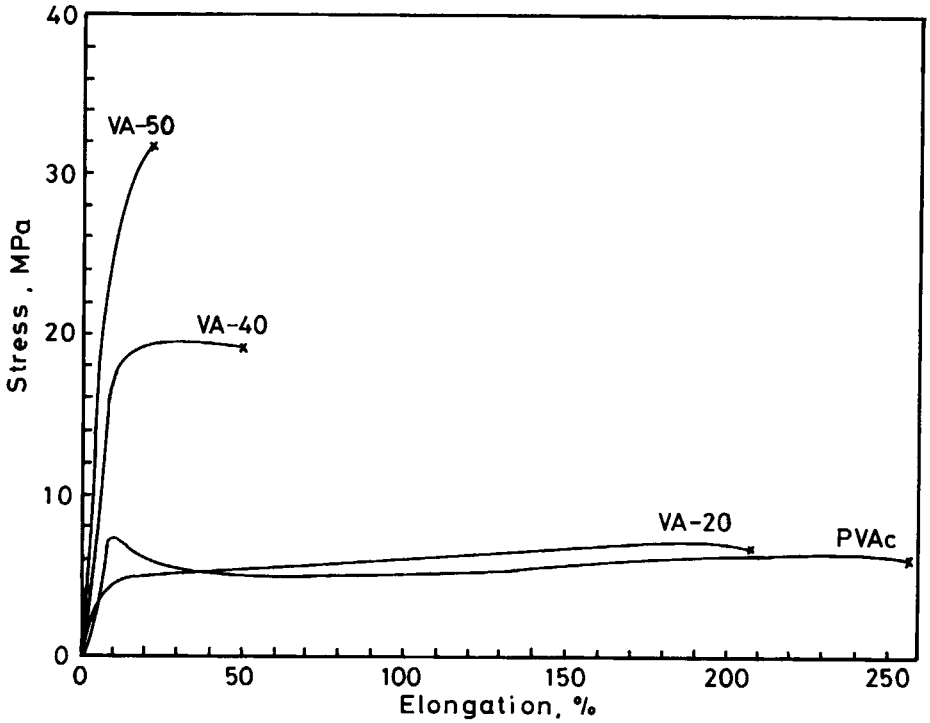

Figure 13 Stress–strain curves of PVAc, VA-20, VA-40, and VA-50.

strength of the CO hybrid was larger than that of VA hybrid due to the difference in their structure.

CONCLUSIONS

PVAc and VAc/VTES copolymer having 10 mol % of ethoxysilane were incorporated into silica gel using the sol–gel process, and the physical properties were compared. In the TG curves of PVAc, copolymers, and hybrids, two-stage degradation processes were observed. The first stage was due to removal of acetic acid from the VAc components, and the second stage was caused by breakup of a $(-C=C-)_n$ chain formed after the first-stage degradation. The residual weights (determined from the TG curve) of the CO hybrids were larger than that of the VA hybrids because the copolymer itself contained a silica component.

The DSC curves of the VA hybrids were complex because of an overlap of the endotherms (which are due to Tg) and the exotherms (which are due to sol–gel reactions). In the DSC curves of the CO hybrids, the exotherms occurred at about 25–27°C and the endotherms at about 73–75°C, which were caused by sol–gel reactions and Tg of the hybrid, respectively.

The dynamic viscoelastic properties of the hybrids were measured as a function of temperature. E' of the hybrids increased with increasing amounts

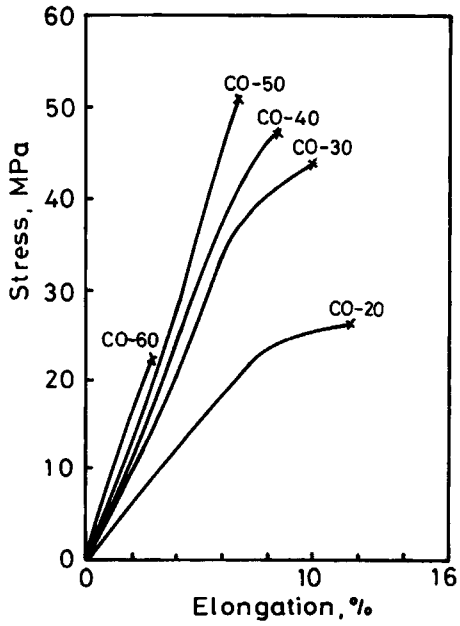

Figure 14 Stress–strain curves of CO-20, CO-30, CO-40, CO-50, and CO-60.

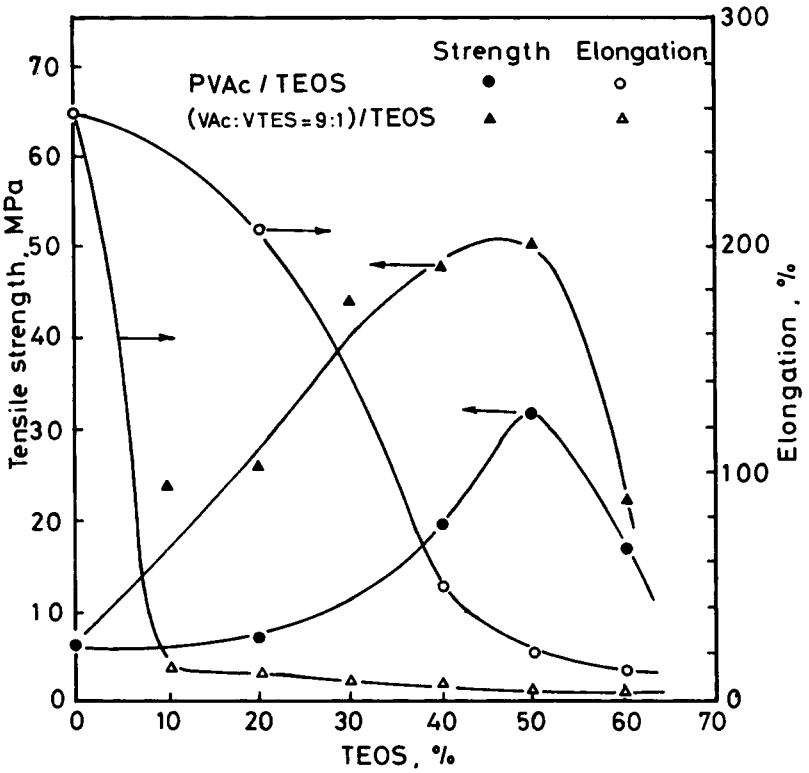

Figure 15 Tensile properties of PVAc-hybrid and copolymer-hybrid as a function of mixed TEOS content.

of TEOS over a wide range of temperature, namely −20 to 120°C. In the E' curve of the VA hybrids, a plateau occurred at 60–80°C and a break point at about 90°C, in contrast to the E' curve of the CO hybrids, which gradually decreased with temperature. In the E'' curves of the VA hybrids, a sharp peak appeared at about 40°C, and is attributed to the glass transition of the hybrid. The position of this peak did not change with TEOS content. An additional shoulder peak was observed at 70 and 90°C for VA-40 and VA-50. The origin of this peak is uncertain at present. The E'' peak of the CO hybrids was broad and its position shifted to a higher temperature when the TEOS content increased.

The tensile strength of the hybrids increased with increasing amounts of TEOS content, and had a maximum at 50 wt % of TEOS. The strength of the CO hybrids (maximum of 50 MPa) was higher than that of the VA hybrids (maximum of 30 MPa). The elongation of the VA hybrids was higher than that of the CO hybrids. The elongation of both hybrids decreased with TEOS content.

The differences in the various physical properties between VA and CO hybrids arise from the difference in the hybrids' structures. Organic polymer molecules in a CO hybrid combined covalently with silica-gel molecules through the VTES component, while a VA hybrid has no bonding between PVAc and silica-gel molecules.

REFERENCES

1. S. Yano, *Bull. Ind. Prod. Res. Inst.*, No. 118, 29 (1991).
2. T. Saegusa, *J. Macromol. Sci.-Chem.*, **A28,** 817 (1991).
3. F. Suzuki, K. Onozato, and Y. Kurokawa, *J. Appl. Polym. Sci.*, **39,** 371 (1990).
4. M. Nandi, J. A. Conklin, L. Salvati, Jr., and A. Sen, *Chem. Mater.*, **3,** 201 (1991).
5. Y.-P. Ning, M.-Y. Tang, C.-Y. Jiang, and J. E. Mark, *J. Appl. Polym. Sci.*, **29,** 3209 (1984).
6. P. Xu, S. Wang, and J. E. Mark, *Mat. Res. Soc. Symp. Proc.*, "Better Ceramics Through Chemistry IV", 180, 445 (1990).
7. S. Wang, P. Xu, and J. E. Mark, *Rubber Chem. Technol.*, **64,** 746 (1991).
8. D. Ravaine, A. Seminel, Y. Charbonillot, and M. Vincens, *J. Non-Cryst. Solid,* **82,** 210 (1986).

9. B. Wang and G. L. Wilkes, *J. Polym. Sci.: Polym. Chem.*, **29,** 905 (1991).
10. P. H. Glaser and G. L. Wilkes, *Polym. Bull.*, **22,** 527 (1989).
11. H.-H. Huang, G. L. Wilkes, and J. G. Carlson, *Polymer,* **30,** 2001 (1989).
12. A. B. Brenan and G. L. Wilkes, *Polymer,* **32,** 733 (1991).
13. K. A. Mauritz and C. K. Jones, *J. Appl. Polym. Sci.,* **40,** 1401 (1990).
14. E. J. A. Pope, M. Asami, and J. D. Mackenzie, *J. Mater. Res.,* **4,** 1018 (1989).
15. I. D. Stefanithis and K. A. Mauritz, *Macromolecules,* **23,** 2397 (1990).
16. K. Nakanishi, N. Soga, H. Matsuoka, and N. Ise, *J. Am. Ceram. Soc.,* **75,** 971 (1992).
17. H. Matsuoka, S.-R. Chen, H. Ishii, N. Ise, K. Nakanishi, and N. Soga, *Bull. Chem. Soc. Jpn.,* **64,** 1283 (1991).
18. A. Morikawa, Y. Suzuki, M. Kakimoto, and Y. Imai, *Polym. Prepr. Jpn.,* **40,** 311 (1991).
19. H.-H. Huang, G. L. Wilkes, and J. G. Carlson, *Polymer,* **30,** 2001 (1991).
20. J. L. W. Noell, G. L. Wilkes, D. K. Mohanty, and J. E. McGrath, *J. Appl. Polym. Sci.,* **40,** 1177 (1990).
21. K. Honda, M. Fujita, H. Ishida, R. Yamamoto, and K. Ohgaki, *J. Electrochem. Soc.;* Solid-State Sci. Technol., **135,** 3151 (1988).
22. M. Fujita and K. Honda, *Polym. Commun.,* **30,** 200 (1989).
23. *Polymer Handbook Second Edition,* J. Brandrup and E. H. Immergut, Eds. Wiley, New York, 1975, p. VI-15.
24. ibid, pp. II-387–II-404.
25. F. W. Billmeyer, Jr., *Textbook of Polymer Science,* Wiley, New York, 1962, Chap. 11.
26. I. C. McNeill, *J. Polym. Sci.,* Part A-1, **4,** 2479 (1966).
27. M. Gordon and J. S. Taylor, *J. Appl. Chem.,* **2,** 493 (1952).
28. T. G. Fox, *Bull. Am. Phys. Soc.,* **1,** 123 (1956).
29. L. Mandelkern, G. M. Martin, and F. A. Quinn, *J. Research Natl. Bur. Standards,* **58,** 137 (1957).
30. L. A. Wood, *J. Polym. Sci.,* **28,** 319 (1958).

Received August 9, 1993
Accepted March 11, 1994